EUROfusion

WPPFC-PR(17) 17551

T Bilyk et al.

Molecular dynamics simulations of helium bubble growth in tungsten

Preprint of Paper to be submitted for publication in
Nuclear Materials and Energy

This work has been carried out within the framework of the EUROfusion Consortium and has received funding from the Euratom research and training programme 2014-2018 under grant agreement No 633053. The views and opinions expressed herein do not necessarily reflect those of the European Commission.

Molecular dynamics simulations of helium bubble growth in tungsten

T. Bilyk[a,*], C. Björkas[a], K. Nordlund[a], E. Safi[a]

[a] *EURATOM/Tekes, Department of Physics, P.O. Box 43, FI-00014 University of Helsinki, Finland*

Abstract

Due to its exceptional high temperature properties tungsten is the most promising material for the divertor in ITER and future tokamak reactors. However, a puzzling tendril-like nanostructure, called W fuzz, has been observed at the surface of tungsten after He irradiation under reactor-specific conditions. Previous simulations provide a partial explanation about the formation of this nanostructure with the help of certain helium cluster distributions, however atomic details of these are not clear. In this work, these distributions are investigated using molecular dynamics (MD), shedding light into how they are affected by the initial vacancy concentration and temperature. The results support assumptions made in previous MD and Monte-Carlo studies about the fuzz formation.

Keywords: Fusion materials, tungsten, molecular dynamics simulations, Helium, clustering

*Corresponding author

Email address: thomas.bilyk@gmail.com (T. Bilyk)

1. Introduction

Tungsten (W) has been chosen as the main divertor plate material in the ITER fusion reactor [1], due to its superior qualities regarding sputtering yield, melting temperature, thermal conductivity and tritium retention [2, 3]. The requirements are rigorous, since the divertor environment is extremely harsh, as waste materials and impurities are removed out of the reactor through the divertor during operation. In addition, large areas will be exposed to high fluxes of low energy hydrogen (H) and helium (He) ions [4, 5]. During laboratory experiments trying to mimic realistic reactor conditions ($T_{\mathrm{W}} = 900 - 2000$ K and $E_{\mathrm{He}} < 100$ eV) a tendril-like nanostructure, so-called "W fuzz", has been observed to form at the surface of tungsten [5].

Many theoretical and modelling studies have been performed to elucidate the mechanisms behind the W fuzz formation. For instance, the interactions between He and W have been studied using Density Functional Theory (DFT) (e.g. References [6, 7, 8]), providing insight into the binding and migration of intrinsic He point defects in bulk W. Molecular dynamics (MD), on the other hand, has been used to investigate the influence of He on the properties of W and elementary processes that lead to a fuzzy nanostructure. For instance, Sefta et al. [9] showed that a high pressure in subsurface bubbles leads to a series of loop punching processes, bringing the bubble closer to the surface. Depending on the size of the bubble, it could either burst and crater the surface, or create a pinhole link to the surface so that He is able to escape from the substrate, a process first reported by Henriksson et al. [10]. Another study by Sefta et al. [11] showed that He subsurface nanobubbles do not have a significant influence on the W sputtering yield. Furthermore, the simulations of Juslin and Wirth [12] showed that H may be trapped in He

bubbles, leading to an increase in the H retention W when He is present. MD simulations combined with experiments and SRIM [13] simulations were realised by Pentecoste et al. [14], small systems under high flux of He were observed to release W flakes into the plasma. Also Monte Carlo (MC) techniques have been employed, e.g. Ito et al. [15] combined DFT and hybrid MD-MC simulations and proposed a four-step process to explain the fuzz formation. Lasa et al. [16] combined MD and object kinetic MC and were able to reproduce the time dependence on the fuzz formation. Most recently, Valles et al. have proposed an explanation for the temperature dependence on the process, using MC simulations [17].

None of the above studies make an attempt to explain the temperature dependence on the bubble distribution. In the present study we use MD simulations in an attempt to give an explanation for the He clustering in bulk W at short time scales, focusing on how different temperatures and vacancy concentrations lead to different cluster distributions.

2. Method

The MD simulations were performed using the PARCAS code [18]. The interactions between tungsten atoms were described using the Finnis-Sinclair N-body potential [19], as modified by Ackland-Thetford [20] and adjusted for short range interactions by Juslin et al. [21]. W-He interactions were described using the potential of Juslin et al. [21], and the He-He interactions by Beck's potential [22] as modified at short ranges by Morishita *et al* [23]. In all simulations, the starting point simulation cell consisted of a $10 \times 10 \times 10$ body-centered cubic (BCC) lattice of 2000 tungsten atoms, in which He atoms were added and W atoms removed randomly according to desired initial configuration. Periodic boundaries

Table 1: Summary of performed simulations, with N_V, the initial number of vacancies; $\%_{He}$, the percentage of helium atoms present in the simulation compared to the initial amount of tungsten atims and $N_{simulations}$, the number of different separate simulation starting configurations at each temperature, used for statistics.

Set	N_V	$\%_{He}$	Temperature (K)	Simulation time (ns)	$N_{simulations}$
1	0, 1, 3	1	300, 1000, 2000	2	20
2	0, 1, 3	1, 3	300, 500, 700, 900, 1000	2	10
3	0	3	700, 900, 1000, 1500	30	30
4	0	3	2000	30	2

were used in all directions. Berendsen's thermostat [24] was used to set temperature, then microcanonical dynamics were used. For statistics, several runs for the same temperature were performed, each run starting from a unique configuration. A summary of the different simulations is given in Table 1.

The analysis of tungsten positions in order to extract vacancies and interstitial positions was done by a Wigner-Seitz cell method. For the cluster analysis, the convention was to count two entities to the same cluster if they were closer than 2 Å. This somewhat arbitrary condition was checked visually for several cases and it was deemed good.

3. Results and discussion

The results of the study are in a general agreement with the MC simulations of Valles et al. (”At low temperatures (700 K), the great majority of He atoms are re-

tained in monovacancies (He_nV_1 clusters), which remain stable. At intermediate temperatures (900-2000 K), He atoms are retained inside larger He_nV_m clusters, which grow to form fuzz-like structures."). Here we showed that at low temperatures helium atoms are mainly trapped in small He_nV_m clusters with $m < 4$, when at high temperatures, large clusters are able to form due to faster diffusion of He_n clusters.

3.1. Influence of vacancy concentration on the clustering

Figure 1 shows the final cluster distributions after 2 ns at a substrate temperature of 300 K and 1000 K from run sets 1-2 in Table 1. The results of each graph is averaged over 10 runs. The graphs illustrate the number of clusters in the simulation box as a function of the different number of He (n) and vacancies (m) in the clusters. The first graph, Figure 1 a), presents the distribution for a substrate temperature of 300 K, and is a typical example of the behaviour of a cluster distribution in the presence of vacancies: a higher initial vacancy concentration means fewer clusters without vacancies (V_0), and more small size clusters (such as V_1) at the end of the simulation.

This graph also shows that large clusters (bubbles) are not favoured by a higher initial vacancy concentration. In fact, the opposite is observed in Fig. 1 b), presenting the cluster distribution in a substrate at 1000 K : a higher vacancy concentration leads to more small V_1 clusters across the lattice, and therefore less larger ones. This graph also highlights the fact that after 2 ns at a high temperature, the quantity of diffusing V_0 clusters is low, whereas at a lower temperature such as 300 K, the slow diffusion of these clusters prevents their encounter and the formation of $V_{m\geq 1}$ clusters, so some movement can still be observed. This observation means that the steady distribution of clusters is almost reached af-

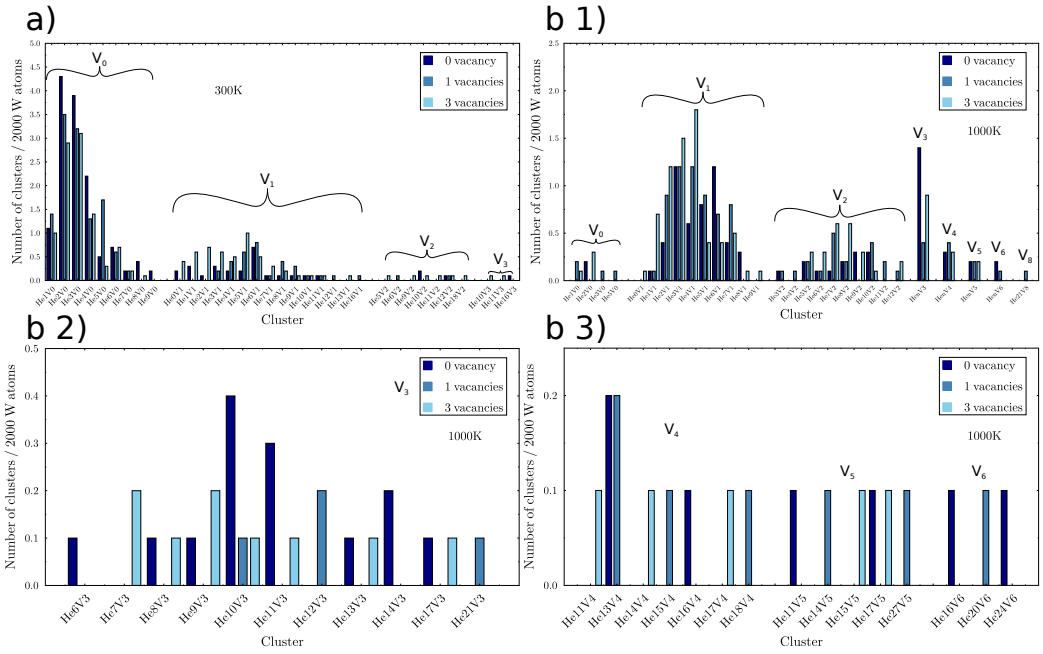

Figure 1: Distributions of V_m clusters in tungsten lattice containing 60 helium atoms, after 2 ns for a substrate temperature of a) 300 K and b) 1000 K (split up in three parts for clarity). The dark blue correspond to a lattice with initially 0 vacancies; medium blue to 1 initial vacancy and light blue to 3 initial vacancies. The simulations correspond to the set 2 of the 1.

ter 2 ns at 1000 K, if we consider the hypothesis that only V_0 clusters are mobile [25, 26, 27]. The presence of $He_{7\rightarrow9}V_0$ clusters at 300 K is also interesting and will be discussed further in the next section.

The increase of small V_1 clusters and the decrease of large ones can be explained by vacancies acting as traps for surrounding helium atoms. Clusters are able to grow around vacancies (and also without them due to the high binding energy between helium atoms [28, 21, 7]). The calculations of Becquart [7] showed that the migration energy of a single W vacancy is about 1.66 eV, meaning that the clustering of helium atoms around vacancies leads to a decreasing mobility of

helium in tungsten. As an example, a simulation of a lattice with 249 tungsten atoms, one vacancy and one helium atom in a substitutional position (He_1V_1 cluster) showed that even at 1500 K, this He_1V_1 cluster did not move during a whole nanosecond.

The binding energy of He to a V_m cluster corresponds to the barrier energy for He to leave the cluster. The high value of this binding energy ($E_b(\mathrm{He}-\mathrm{He}_n\mathrm{V}_m) > 2$ eV [21] for the potentials used) guarantees the stability of the clusters and the corresponding He retention in V_m clusters. According to Ito et al. [15], the migration energy for a He cluster containing a mono-vacancy is about 3.07 eV, showing that for short times (nanosecond scale), the cluster growth process cannot be due to the migration of V_m clusters. Helium atoms are then trapped in small clusters with vacancies, which are spread randomly in the lattice. An initial vacancy concentration thus offers more nucleation points for clusters, meaning that helium atoms cluster in a more homogeneous way in the lattice and therefore the amount of bubbles is reduced.

3.2. Influence of the temperature on the clustering

For the simulations in the following part (run sets 3-4, i.e. without initial vacancies), 30 runs were performed for each temperature and the results are averaged over these. Figure 2 shows the number of clusters as a function of vacancy size for different temperatures after 30 ns. The tendency is mainly the same for all temperatures: most of the clusters are V_1, and the more vacancies a cluster contains, the rarer it is. Details of the final cluster distributions after 30 ns at different temperatures are shown in Fig. 3.

Figs. 2 and 3 show several things. First, mobile vacancy-free clusters with more than 3 He were rare at the end of the simulations. The formation of a Frenkel

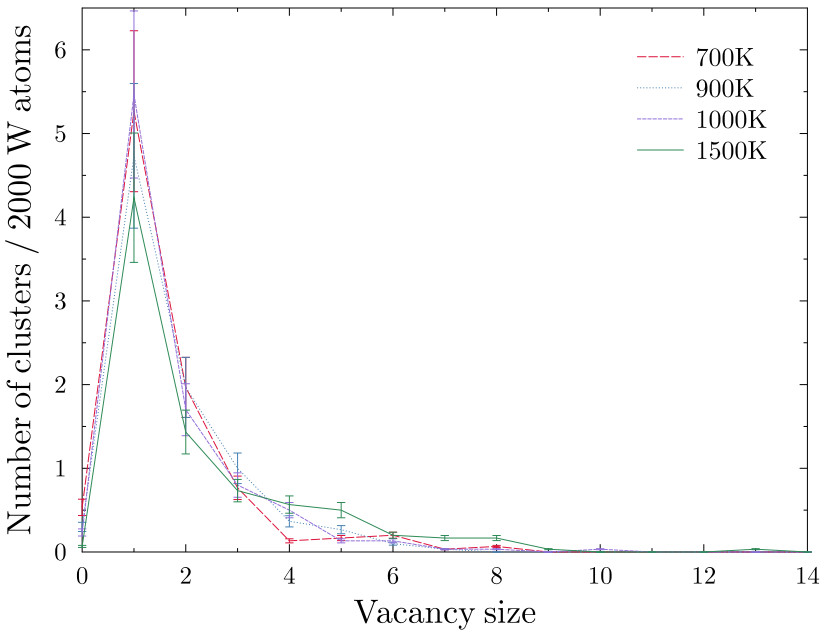

Figure 2: Distribution of clusters by vacancy size, after 30 ns at different temperatures, set 3 of the 1. Error bars represent the standard error.

pair should appear with 5 to 7 He atoms in the clusters, as discussed in [27] and lower. It may be surprising that bigger moving clusters weren't observed, however temperature help diffusion, i.e. cluster growth. Second, the number of clusters containing only one vacancy seems to decrease with increasing temperature, in favour of clusters with more vacancies. The increasing number of helium in a cluster lead to an increase in the pressure exercised by the cluster on the surrounding lattice, which deforms itself [10]. This pressure, helped by the thermal activation leads to Frenkel pair formation. This process, called "trap mutation",

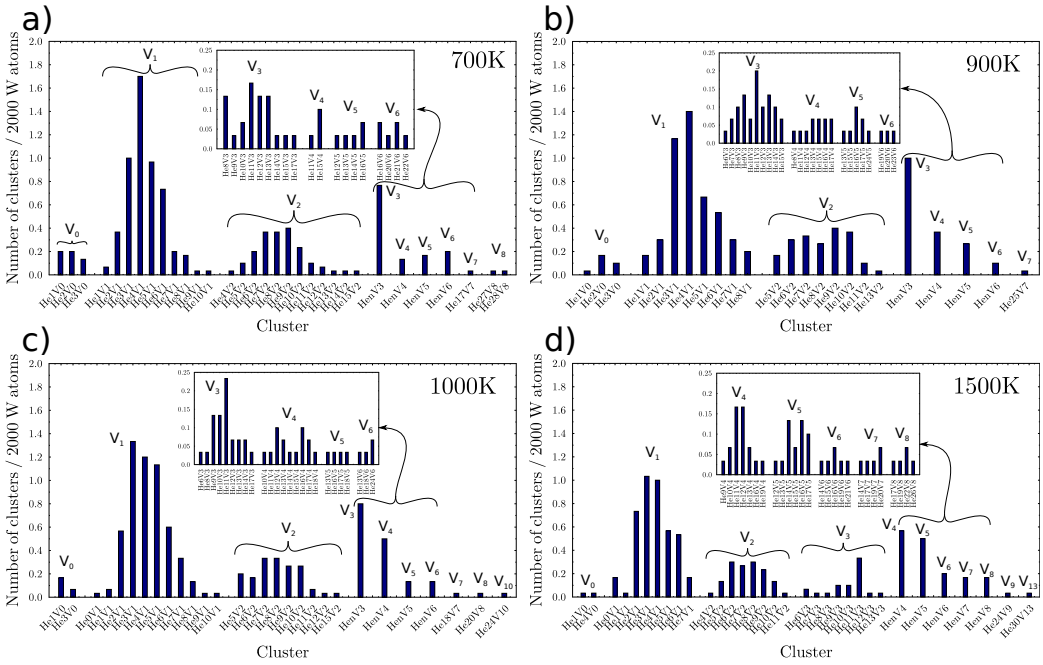

Figure 3: Distribution of clusters in a lattice containing 2000 W and 60 He atoms, after 30 ns and at a) 700 K b) 900 K c) 1000 K and d) 1500 K. The insets show the distributions for large clusters. The simulations correspond to the set 3 of the 1

increases the number of vacancies in the cluster and moves tungsten atom to a self interstitial crowdion $< 111 >$ position [7].

Third, the number of V_2 and V_3 clusters also decreases with temperature. Helium atoms gather in larger clusters (bubbles), therefore less clusters are observed at high temperatures. A few $V_{m\geq 4}$ bubbles were seen to contain as much helium atoms as some $V_{m\leq 3}$ clusters. Bubbles with five or more vacancies can contain a large range of helium atoms (e. g. at 900 K, n in He_nV_5 clusters goes from 13 to 24). Thus, the probability to obtain two large bubbles with the same composition is smaller than for two small ones. These two facts explain the different shapes of

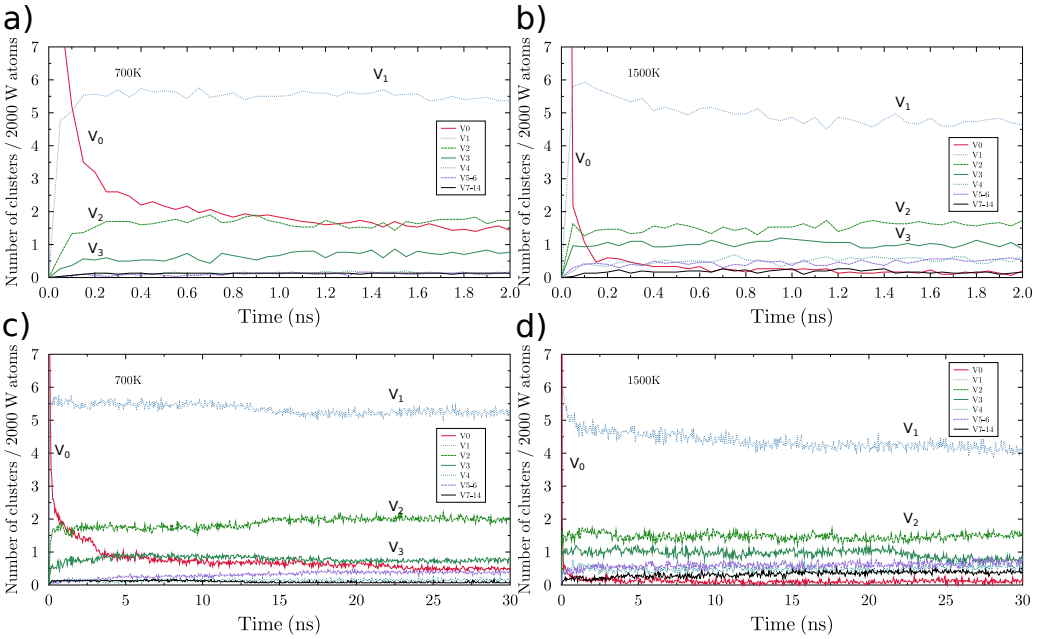

Figure 4: Evolution of clusters by vacancy-size for 2 and 30 ns at a,c) 700 K and b,d) 1500 K. The zoom in to the first 2 ns is shown since most development takes place during the first 2 ns. Sets 3 of the 1

.

the distribution when the temperature changes.

Figure 4 shows the evolution of clusters sorted by their number of vacancies at 700 K and 1500 K to compare the differences between low and high temperatures, both for 2 ns and 30 ns. This time separation was done to highlight that the cluster distribution should obtain its final shape already at an early stage, because it is mainly due to fast V_0 diffusion. Indeed, for each temperature, the number of V_0 clusters has the form of a decreasing exponential. The 2 ns graphs show that the convergence is faster with higher temperature and the final remaining V_0 clusters also decreases with higher temperature. This means that the steady distribution of

clusters is reached faster at high temperatures, which is natural considering that the bubble growth is governed by diffusion and trapping of V_0 clusters.

The main evolution is observed to take place in the first nanoseconds (hence the zoom in this part). For each temperature, the number of V_1 clusters experiences a jump in the beginning of the simulation and tends to slow down in two ways. First, in the 2 ns graphs, a peak appears for high temperatures. Second, in the 30 ns graphs, a slow decreasing tendency is observed. The final number of V_2 clusters is higher at low temperatures (700 K and 900 K). The final number of V_3 was observed to be higher at 1000 K. Finally, the number of large clusters ($m > 4$) increases with temperature. After the first 2 ns step, some noteworthy events such as the ones at 13 ns for 700 K or 22 ns for 1500 K were observed. These events correspond to the coalescence of V_m clusters in close proximity, and are rare events especially at high temperatures.

The temperature dependence on the distribution of V_m is mainly due to the clustering during the two first nanoseconds. The next paragraphs will discuss the processes during that time.

As the helium migration energy in tungsten is between 0.06 to 0.15 eV according to DFT simulations [7, 27], helium is mobile even below 5 K [29]. The high self-binding energy of helium and the low migration energy lead to a fast so called first step, which correspond to the first few ps of the simulations performed. During this first step, helium atoms gather with surrounding He to form small vacancy-free mobile clusters ($He_n \sim 4$). The higher the substrate temperature, the faster the diffusion of He_n, which results in a larger diffusion range of these clusters.

During the second step (some picoseconds to around 1 ns), these clusters dif-

fuse and their diffusion rates depend on the temperature. The coalescence of these vacancy-free clusters form larger V_0 clusters that become unstable if they contain too much He. This limit is investigate lower and was observed to depend on the temperature, going from 6-7 He at 700 K to 5-6 at 1000 K. At low temperatures (300 K), also He_6 and He_9 clusters were present (Figure 1).

These unstable clusers excert a high pressure on the surrounding lattice, which, along with thermal activation, leads to Frenkel pair formation, increasing the space occupied by the cluster and releasing the constraint excerted on the surrounding lattice. This process leads to the formation of an immobile V_1 cluster. Once a cluster with a vacancy is formed, two growth processes are available: Coalescence with other close and immobile clusters or trapping with V_0 clusters that are diffusing next to it. During the first hundreds of picoseconds, clusters can grow with these processes. The first one is possible if two clusters emerge close to each other, their growth reduces the distance between them and can lead to coalescence in the beginning of the simulation. This process should be distinguished from bubble coalescence after a certain steady distribution appears in the lattice. In that case, bubbles can be considered as trapped at their positions in the time range considered in this work. The high binding energy of helium with clusters [21] ensures that a V_0 cluster near a cluster is trapped. The growth by these two processes continues to increase the amount of helium in the clusters, leading to a pressure increase and subsequent Frenkel pair formation.

The observation made about V_1 clusters in the last section along with this analysis tend to affirm that bubble growth in tungsten is mainly governed by the migration of fast diffusing V_0 clusters. Therefore the temperature dependence on the cluster distribution should be explainable by considering the differences in the

diffusion of these clusters at different temperatures.

At low temperatures, the slow diffusion of V_0 clusters reduces their diffusion range and leads to the creation of small clusters across the lattice. The growth opportunity of V_0 clusters is reduced to the encounter with other similar clusters or emerging clusters that are developing in their short diffusion range. This way, the lattice can be seen as small areas that are occupied by small growing V_m clusters, the growth of which is ensured by trapping close, small and low mobility V_0 clusters. The result is a lattice with a nearly homogeneous repartition of small and medium size clusters with a few remaining V_0 clusters due to their slow diffusion. In this final distribution, the clusters are close to each other, but their high migration energies limit the chances of coalescence. The 2 ns simulations illustrated in Fig. 4 support this cluster formation hypothesis. Indeed, at low temperatures, the number of V_1 clusters rauses furst rapidly and then decreases slowly by trapping V_0 clusters and forming V_2 clusters. At high temperatures, the V_1 rise is smaller, because the formation of large clusters happens faster and gathers more helium atoms that do not end up in emerging small clusters. The V_1 peak corresponds to the growth of these clusters, as the decrease of V_0 and the increase of larger cluster curves are coordinated with it. High temperatures increase the diffusion range of helium atoms and V_0 clusters, increasing their chances to meet a V_m cluster before being trapped and slowed down in another V_0 cluster. At these temperatures, the number of diffusing clusters decreases fast and the final distribution of clusters is thus reached faster.

To sum up, the growth of the first emerged clusters is favoured at high temperatures, and the emergence of small ones is favoured at low temperatures. After the two first fast steps of a simulation (less than 1 ns), a certain steady distribution

is reached, and the only growth processes hereafter are the trapping of the few remaining V_0 that are still moving in the lattice, or the coalescence of clusters in close proximity. These processes reduce in amount faster at high temperature, the first one because high temperature aids the diffusion of V_0 clusters during the first steps and hence the encounter of growing clusters; the second one because the temperature favours the formation of large distant bubbles.

The last conclusion should be nuanced, indeed the Figure 2 showed that the distribution of clusters by vacancy size is mainly the same for different temperatures : a major part of V_1 clusters and a few larger ones. This tendency reveals that the main process that happens is the encounter of closeby helium V_0 clusters leading to trap mutations, for all temperatures. Temperature simply helps a few V_0 clusters to reach growing clusters before coalesces with other helium clusters. The distributions observed contain some V_1 clusters spread out all over the lattice with a few larger clusters here and there. Their size and number depend on temperature.

Figure 5 illustrates the cluster distribution by the ratio of helium atoms to vacancies in the clusters. Fig. 5 a) displays the distribution by ratios for $He_nV_{m\leq 2}$ clusters. It highlights the fact that high ratios are due to relatively small ($m \in \{1;2\}$) clusters and shows distinct peaks at integer numbers and smaller peaks, but still distinguishable at half-integer ratio, respectively corresponding to $V_1 - 2$ and V_2 clusters. The profiles of integer and half-integer ratios show that for small clusters, a stable configuration is with a $\frac{n}{m}$ ratio between 2 and 6. The clusters corresponding to the ratios out of this interval are metastable ones. Temperature seems to decrease the ratio, which is a direct consequence of ideal gas law : $PV = Nk_BT$. Fig. 5 b) also illustrate the distribution by ratio, counting only clusters

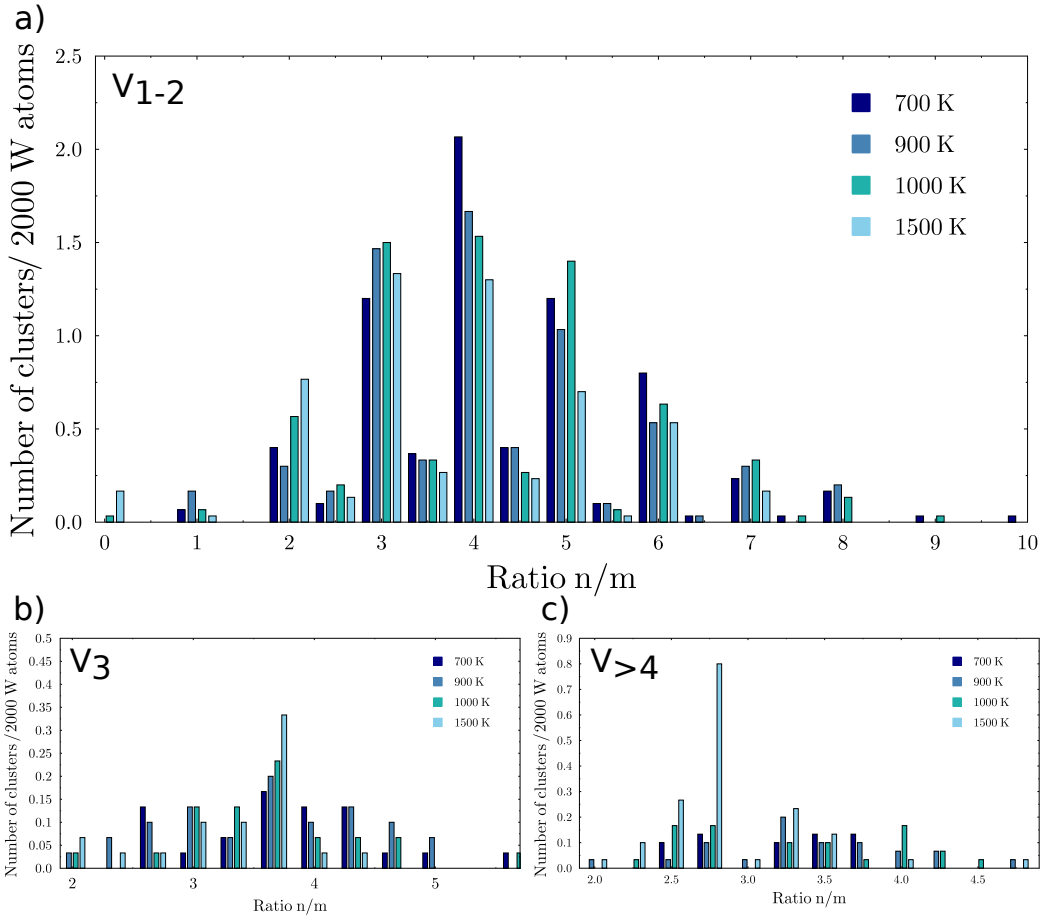

Figure 5: Ratio $\frac{n}{m}$ in the formed clusters for different temperatures. n is the number of helium atoms and m the number of vacancies in the cluster. a) Clusters with 1 or 2 vacancies b) clusters with 3 vacancies and c) clusters with 4 or more vacancies.

with 3 vacancies. The statistics begin to be poor at these points (not that much v_3 clusters), but this graph also shows that a high temperature tends to lower the ratio.

Fig. 5 c) shows the same distribution for $He_nV_{m\geq 4}$ clusters. It illustrates as before that a high temperature favours lower ratios. An explanation could be that

the pressure exercised by the clusters is sided by the thermal energy to form of a Frenkel pair and thus lower the ratio $\frac{n}{m}$.

This hypothesis was investigated by determining the n-limit value that leads to a Frenkel pair formation by a V_0 cluster at two different temperatures, 700 K and 1000 K. The simulations were done in the following way. He atoms were added one by one into a W lattice of same size as in the above mentioned simulations. It was checked that no He atom was placed too close to another atom. The next He atom was only added after the previous ones were gathered together in the same cluster. A few nanoseconds of simulations at different temperatures were done to investigate the stability of the clusters. At 700 K, the strain exerced by a He_6 cluster pushed an atom on the next Wigner-Seitz cell for a single time step, suggesting that the He_6 cluster is stable at 700 K. The following He_7 cluster became a stable He_7V_1 cluster 500 ps after its formation (He_6+He$\rightarrow He_7$), adding a single atom to a He_6V_0 cluster caused trap mutation.

At 1000 K, two similar short-lived Frenkel pairs were observed for the He_5 cluster, during the 2 ns following the formation of the cluster. The He_6 cluster formed a stable Frenkel pair 77 ps after its formation. Fig. 1 a) shows that at 300 K, the thermal activation may be too low to form a Frenkel pair by a He_9 cluster.

These observations support the previous hypothesis and explain how a high temperature lowers the ratio $\frac{n}{m}$, giving more space for clusters to create large bubbles.

Figure 5 c) also shows that for bubbles, the ratio $\frac{n}{m}$ is lower than 5. It seems that large clusters tends to lower the ratio compared to Fig. 3. A large amount of helium atoms in the bubble gives a constant pressure on the surrounding lattice, which stabilizes the bubble by forming Frenkel pairs. If the pressure is high

enough, the thermal activation may play a less important role in Frenkel pair formation, as discussed recently by Sandoval et al. [30, 31].

4. Discussion and conclusions

The main ambition of this study was to investigate the temperature and vacancy concentration dependence on the helium cluster distribution in bulk tungsten.

It was observed that vacancies tend to increase the formation of new clusters, and therefore favour a distribution with small and medium clusters and only rare large bubbles. This can be explained by the fact that vacancies act like traps for mobile helium, and since the binding energy between a He atom and a $\mathrm{He}-\mathrm{He}_n\mathrm{V}_m$ cluster is high, once the helium atom is trapped, it stays trapped. As the migration energy of V_m clusters is high, their growth cannot be ensured by coalescence, hence the major growth process is trapping of diffusing helium atoms.

It was also observed that low temperatures lead to a large amount of small and medium immobile clusters homogeneously distributed in the lattice, and high temperatures lead to a few large bubbles and some medium sized clusters. The temperature promotes diffusion of small V_0 clusters in the beginning of the simulation, and a fast diffusion increases their chances to reach a growing large cluster, reducing events of coalescence with others V_0 clusters that lead to emergence of small clusters. This explains why different temperatures lead to different cluster distribution, and also why the final distributions were seen to be shaped during the first hundreds of picoseconds of a simulations, when vacancies appear by trap mutation. After the first fast diffusion processes and coalescence events, the growth of V_m clusters is ensured by trapping the remaining diffusing He_n clusters. Rare

coalescence of close-by clusters were observed, but studies investigating diffusion of large bubbles on longer time scales are needed to confirm that the coalescence of large bubbles could also modify the distribution.

By irradiating tungsten surfaces, a similar process could happen. The diffusion range of helium atoms between two irradiation events also depends on the substrate temperature. Therefore, at low temperatures, a slow diffusion of helium atoms would lead them to bond with new irradiating atoms that arrive in close vicinity to them, thus favouring the formation of new small clusters. High temperatures, on the other hand, increase the diffusion range of helium atoms and clusters, enabling them to find growing clusters before clustering with newly irradiating atoms. When an steady state is reached, low temperatures could reveal some well distributed small clusters, while high temperatures could result in additional large ones. The continuity aspect of irradiation (helium incoming one by one) compared to bulk simulations, should lead to help incoming He to reach a growing cluster. Therefore, the resulting bubbles due to irradiation should be larger than the ones observed in this study. (This is in good agreement with the assumption made in MD and MC studies[12, 15, 17] that investigate helium bubble burst and the formation of tungsten fuzz.) These remarks should be investigated with irradiation simulations.

5. Acknowledgements

This work has been carried out within the framework of the EUROfusion Consortium and has received funding from the Euratom research and training programme 2014-2018 under grant agreement No 633053. The views and opinions expressed herein do not necessarily reflect those of the European Commission.

Funding from the ERASMUS grant Ref ES 15-16-000168 were also received.

References

[1] ITER Physics Basis Editors and ITER Physics Expert Group Chairs and Co-Chairs and ITER Joint Central Team and Physics Integration Unit, Iter physics basis, Nuclear Fusion 39 (1999) 2137 – 2638.

[2] H. Bolt, V. Barabash, W. Krauss, J. Linke, R. Neu, S. Suzuki, N. Yoshida, A. U. Team, Materials for the plasma-facing components of fusion reactors, Journal of Nuclear Materials 329-333 (Part A) (2004) 66 – 73.

[3] G. Janeschitz, I. JCT, HTs, Plasma-wall interaction issues in iter, Journal of Nuclear Materials 290 - 293 (1) (2001) 1 – 11.

[4] A. U. T. R Neu, E. P. Taskforce, J. E. Contributors, Preparing the scientific basis for an all metal iter, Plasma Physics and Controlled Fusion 53 (12) (2011) 124040.

[5] M. Baldwin, R. Doerner, Helium induced nanoscopic morphology on tungsten under fusion relevant plasma conditions, Nuclear Fusion 48 (3) (2008) 035001.

[6] C. S. Becquart, C. Domain, Migration energy of he in w revisited by ab initio calculations, Physical Review Letters 97 (19) (2006) 196402.

[7] C. S. Becquart, C. Domain, Ab initio calculations about intrinsic point defects and he in w, Nuclear Instruments and Methods in Physics Research Section B 255 (1) (2007) 23 – 26.

[8] G. Valles, C. González, I. Martin-Bragado, R. Iglesias, J. Perlado, A. Rivera, The influence of high grain boundary density on helium retention in tungsten, Journal of Nuclear Materials 457 (2015) 80 – 87.

[9] F. Sefta, N. Juslin, B. D. Wirth, Helium bubble bursting in tungsten, Journal of Applied Physics 114 (1) (2013) 243518.

[10] K. O. E. Henriksson, K. Nordlund, J. Keinonen, Molecular dynamics simulations of helium cluster formation in tungsten, Nucl. Instr. Meth. Phys. Res. B. 244 (2006) 377–391.

[11] F. Sefta, N. Juslin, K. D. Hammond, B. D. Wirth, Molecular dynamics simulations on the effect of sub-surface helium bubbles on the sputtering yield of tungsten, Journal of Nuclear Materials 438 (Supplement) (2013) S493 – S496.

[12] N. Juslin, B. D. Wirth, Molecular dynamics simulation of the effect of subsurface helium bubbles on hydrogen retention in tungsten, Journal of Nuclear Materials 438 (Supplement) (2013) S1221 – S1223.

[13] J. F. Ziegler, M. Ziegler, J. Biersack, Srim-the stopping and range of ions in matter (2010), Nuclear Instruments and Methods in Physics Research B 68 (11-12) (2010) 1818 – 1823.

[14] L. Pentecoste, P. Brault, A.-L. Thomann, P. Desgardin, T. Lecas, T. Belhabib, M.-F. Barthe, T. Sauvage, Low energy and low fluence helium implantations in tungsten: Molecular dynamics simulations and experiments, Journal of Nuclear Materials 470 (1) (2015) 44 – 54.

[15] A. M. Ito, A. Takayama, Y. Oda, T. Tamura, R. Kobayashi, T. Hattori, S. Ogata, N. Ohno, S. Kajita, M. Yajima, Y. Noiri, Y. Yoshimoto, S. Saito, S. Takamura, T. Murashima, M. Miyamoto, H. Nakamura, Hybrid simulation research on formation mechanism of tungsten nanostructure induced by helium plasma irradiation, Journal of Nuclear Materials 463 (1) (2015) 109 – 115.

[16] A. Lasa, S. K. Tahtinen, K. Nordlund, Loop punching and bubble rupture causing surface roughening - a model for w fuzz growth, EPL (Europhysics Letters) 105 (2) (2014) 25002.

[17] G. Valles, I. Martin-Bragado, K. Nordlund, C. B. A. Lasa, E. Safi, J. M. Perlado, A. Rivera, Temperature dependence of underdense nanostructure formation in tungsten under helium irradiation, New J. Physics.Submitted for publication.

[18] K. Nordlund, PARCAS computer code. The main principles of the molecular dynamics algorithms are presented in [32, 33]. The adaptive time step and electronic stopping algorithms are the same as in [34] (2006).

[19] M. W. Finnis, J. E. Sinclair, A simple empirical n-body potential for transition metals, Philosophical Magazine A 50 (1) (1984) 45 – 55.

[20] G. J. Ackland, R. Thetford, An improved n-body semi-empirical model for body-centred cubic transition metals, Philosophical Magazine A 56 (1) (1987) 15 – 30.

[21] N. Juslin, B. Wirth, Interatomic potentials for simulation of he bubble formation in w, Journal of Nuclear Materials 432 (1 - 3) (2012) 61 – 66.

[22] D. E. Beck, A new interatomic potential function for helium, Journal of Nuclear Materials 14 (4) (1967) 311 – 315.

[23] K. Morishita, R. Suganoa, B. D. Wirth, T. D. de la Rubiab, Thermal stability of heliumvacancy clusters in iron, Nuclear Instruments and Methods in Physics Research Section B 202 (1) (2003) 76 – 81.

[24] H. J. C. Berendsen, J. P. M. Postma, W. F. V. Gunsteren, A. DiNola, J. R. Haak, Molecular dynamics with coupling to an external bath, The Journal of Chemical Physics 50 (1) (1984) 3684 – 3690.

[25] L. Hu, K. D. Hammond, B. D. Wirth, D. Maroudas, Dynamics of small mobile helium clusters near tungsten surfaces, Surface Science 626 (2014) L21 – L25. doi:http://dx.doi.org/10.1016/j.susc.2014.03.020.
URL http://www.sciencedirect.com/science/article/pii/S0039602814000867

[26] K. D. Hammond, B. D. Wirth, Crystal orientation effects on helium ion depth distributions and adatom formation processes in plasma-facing tungsten, Journal of Applied Physics 116 (14) (2014) 143301.

[27] D. Perez, T. Vogel, B. P. Uberuaga, Diffusion and transformation kinetics of small helium clusters in bulk tungsten, Phys. Rev. B 90 (2014) 014102. doi:10.1103/PhysRevB.90.014102.
URL http://link.aps.org/doi/10.1103/PhysRevB.90.014102

[28] K. O. E. Henriksson, K. Nordlund, A. Krasheninnikov, J. Keinonen, Differ-

ences in hydrogen and helium cluster formation, Appl. Phys. Lett. 87 (2005) 163113.

[29] A. S. Soltan, R. Vassen, P. Jung, Migration and immobilization of hydrogen and helium in gold and tungsten at low temperatures, Journal of applied physics 70 (2) (1991) 793 – 797.

[30] L. Sandoval, D. Perez, B. P. Uberuaga, A. F. Voter, Competing kinetics and he bubble morphology in w, Physical Review Letters 114 (10) (2015) 105502.

[31] L. Sandoval, D. Perez, B. P. Uberuaga, A. F. Voter, Growth rate effects on the formation of dislocation loops around deep helium bubbles in tungsten, Fusion Science and Technology 71 (2017) 1–6. doi:10.1103/PhysRevLett.114.105502.
URL http://link.aps.org/doi/10.1103/PhysRevLett.114.105502

[32] K. Nordlund, M. Ghaly, R. S. Averback, M. Caturla, T. Diaz de la Rubia, J. Tarus, Defect production in collision cascades in elemental semiconductors and fcc metals, Phys. Rev. B 57 (13) (1998) 7556 – 7570.

[33] M. Ghaly, K. Nordlund, R. S. Averback, Molecular dynamics investigations of surface damage produced by kev self-bombardment of solids, Phil. Mag. A 79 (4) (1999) 795.

[34] K. Nordlund, Molecular dynamics simulation of ion ranges in the 1 – 100 kev energy range, Comput. Mater. Sci. 3 (1995) 448.